Analyses of tabulated optical constants for thin films in the EUV range and application to solar physics multilayer coatings

Jennifer Rebellato, Evgueni Meltchakov, Régina Soufli, Sébastien de Rossi, Xueyan Zhang, Frédéric Auchère, Franck Delmotte

Analyses of tabulated optical constants for thin films in the EUV range and application to solar physics multilayer coatings

Jennifer Rebellato[a,b], Evgueni Meltchakov[a], Regina Soufli[a,c], Sébastien de Rossi[a], Xueyan Zhang[d], Frédéric Auchère[d] and Franck Delmotte[a]

[a]Laboratoire Charles Fabry, Institut d'Optique Graduate School, CNRS, Université Paris-Saclay, 91127 Palaiseau cedex, France

[b] Centre National d'Etudes Spatiales, 18 Avenue E. Belin, 31401 Toulouse, France

[c] Lawrence Livermore National Laboratory, 7000 East Avenue, Livermore, California 94550, USA

[d] Institut d'Astrophysique Spatiale, CNRS, Université Paris-Saclay, bât. 121, 91405 Orsay, France

ABSTRACT

The thin film optical constants are key parameters to carry out optical simulation or optimization of multilayer mirrors with high efficiency. However, for most materials, different sets of optical constants can be found in the literature especially in the EUV range, as these parameters are not as well-known in the EUV as in the visible or wavelength range. In this work, we have used several reflectance and transmittance measurements in the wavelength range from 10 nm to 60 nm. Different optical constant files have been tested and compared with the IMD simulation software. We will present some experimental spectra and theoretical simulations to highlight the existing problem on the reliability of optical constants sets and to discuss potential solutions. We focus our research on a few materials of particular interest in the EUV range such as aluminum, aluminum oxide, molybdenum, zirconium, magnesium, silicon carbide, and boron carbide. These analyses lead us to select the most reliable and accurate optical constants set, or to create the best one from the concatenation of existing data for each material of interest.

Keywords: Optical constants, soft X-rays, extreme ultraviolet, EUV, multilayer coatings, solar physics, thin films, materials

1. INTRODUCTION

Many advances have been made in the field of optical thin films in the extreme ultraviolet (EUV) range, defined as the wavelength region from 10 to 60 nm, for solar physics since the first EUV space-borne telescope (SoHO, 1995 [1]). From stacks of periodic nanometer-scale bilayers of optically dissimilar materials to tri-material optical coatings with enhanced performance [2] , new interference coatings have been developed to achieve high efficiency at near normal incidence for imaging and analysis in the EUV [3,4]. Incidentally, the same coatings are also needed in instrumentation for coherent EUV sources and photolithography applications, operating in the same wavelength region.

All these applications required the most accurate optical constants in order to simulate the optical behavior of thin film materials and stacks in response to EUV radiation. In the EUV region, the refractive index n of materials is a complex number expressed as

$$n = 1 - \delta + i\beta, \quad (1)$$

where $(1 - \delta)$ and β represent the dispersive and absorptive portions of the refractive index, respectively. The terms δ and β are known as the optical constants. An alternate representation of optical constants found in the literature (such as the IMD software[5]) is (n, k) where $n=1-\delta$ and $k = \beta$. However, for most materials, different sets of optical constants can be found in the literature [6,7] especially in the EUV range as these parameters are not as well-known as in the visible or infrared radiation range. These mirrors and filters are often designed to operate in the vicinity of their absorption edges, thus making

the lack of optical constants even more noticeable. The absorption edge regions are also where it is most difficult to determine optical constants experimentally, due to the transition from very low to very high absorption, the presence of fine structure and the sensitivity to contamination. Thus, the different values of optical constants found in the literature may imply mistakes and uncertainties in simulations as we illustrate in this paper.

These problems had already been pointed out in former works [7,8] where the authors contributed to list optical constants of several materials over different wavelength ranges and according to different measurements or calculation methods. In this paper, we revisit this problem by including more recent data. We are presenting experimental spectra and theoretical simulations of coatings used for solar physics applications to illustrate the existing problems linked to the optical constants in the EUV range. We are also showing the state-of-the-art optical constants in the EUV from 10 to 60 nm for a few materials of interest in space applications such as aluminum, aluminum oxide, zirconium, magnesium, molybdenum, silicon carbide and boron carbide.

2. SIMULATION AND OPTIMIZATION

2.1. Samples

We have simulated experimental reflectance and transmittance spectra of different optical coatings, using several optical constants files with the IMD software[5]. Comparison of these simulations with reflectivity and transmission measurements on known samples will allow to conclude on the validity of the existing optical constants and to choose the best set of optical constants, to get the most accurate simulations.

We mainly used data from filters and mirrors which have been developed for the Extreme Ultraviolet Imager (EUI) [9] on-board the Solar Orbiter mission (ESA mission to be launched in 2020). The EUI instrument includes two EUV telescopes: the Full Sun Imager (FSI) and the High Resolution Imager (HRI). We consider in this study three aluminum-based band-pass filters and two Al-based multilayer mirrors. The Table 1 presents the name, the structure and the nominal thickness or period d in nanometers of the samples analyzed in this paper. The measurement method, the wavelength range as well as the main actor in the fabrication process of each sample are also shown.

Table 1. Analyzed samples – three filters and two multilayer mirrors - and experiment parameters

Name	Structure	Nominal Thickness (nm)	Measurement	Wavelength range	Fabrication
1829	Al/Zr/Al	50.7/96.3/50.7	Transmission	12 – 27 nm	Luxel
13396	Al/Zr/Al	53.1/92.5/49	Transmission	[12-25 nm] [40-65 nm]	Luxel
1906	Al/Mg/Al	80.1/322.2/80.1	Transmission	12 – 40 nm	Luxel
MP17018	[Al/Mo/SiC]x50 + SiC cap	Period d = 8.9 nm	Reflectometry	15 – 21 nm	Laboratoire Charles Fabry
MP11024	[Al/Mo/B4C]x20	Period d = 16.5 nm	Reflectometry	24 – 36 nm	Laboratoire Charles Fabry

The first three samples in Table 1 are metallic filters provided by the Luxel company for the FSI telescope. The transmittance of the Al/Zr/Al filter (sample 1829) was measured from 12 nm to 27 nm. This filter combined with the dual-band multilayer mirror of the FSI telescope will allow the selection of the Fe X line (17.4 nm). We are also considering the case of the FSI Engineering Test filter (sample 13396) which is similar to sample 1829 and for which the transmittance has been measured on a wider spectral range, up to 64 nm. The Al/Mg/Al filter (sample 1906) was measured on a range of wavelengths from 17 nm to 40 nm. It will allow the selection of the He II line (30.4 nm) when combined with the dual-band mirror coating of the FSI telescope.

We analyzed also two multilayer mirrors (samples MP11024 and MP17018). EUV multilayers mirrors usually consist of a periodic stack of two materials. However, we have demonstrated in the past that the addition of a third material in the period can provide higher reflectivity[10]. In 2009, a B_4C/Mo/Si coating was successfully deposited on the mirror of HECOR coronagraph[11] and became the first three-component periodic multilayer aboard a solar EUV observation mission with the

Herschel NASA sounding rocket. Since then, Al/Mo/SiC periodic and bi-periodic coatings have been selected to be the first three-component mirror aboard a solar EUV observation satellite, Solar Orbiter[3]. In the EUV range, three-component multilayer mirrors showed higher efficiencies[10]. Al/Mo/B_4C and Al/Mo/SiC interference coatings have been developed simultaneously as coating candidates for the Solar Orbiter mission[3]. Despite similar efficiencies at 17.4 nm and 30.4 nm, Al/Mo/B_4C has not been selected mostly because of technical considerations such as the low deposition rate of B_4C and the chamber contamination associated with the sputtering of this material. Furthermore, B_4C presents a higher mechanical stress than SiC. This feature could become a problem considering the extreme conditions Solar Orbiter will endure.

2.2. IMD Simulations

2.2.1. Full Sun Imager filters aboard Solar Orbiter satellite

FSI filters for Solar Orbiter have been provided by the Luxel company according to the specificities required by *the Institut d'Astrophysique Spatiale d'Orsay (IAS),* the lab in charge of the development of the FSI on-board instrument. Their transmittances were measured on the Metrology beamline at SOLEIL Synchrotron[12], except for the FSI Test Engineering 13396 measured at PTB Synchrotron. For each filter, several optical constants data have been tested for Al, Zr, Mg and Al_2O_3 in order to obtain the best fit of the measured transmittance (a comprehensive list of optical constant data sets used is given in section 3). In this section, we present a selection of simulation results to illustrate the influence of the choice of optical data set. As the filters are Al-encapsulated coatings exposed to the atmosphere, we had to consider an aluminum oxide layer for both samples in our simulations. The average thickness of this oxide layer was estimated to be 5 nm which is consistent with the following simulations. This thickness may vary according to the coating fabrication method [8]. An average roughness σ of 0.3 nm rms was also applied at each interface, although the transmission measurement is not very sensitive to this parameter. Indications in parentheses in Table 2 and in Table 4 correspond to experimental thickness values which differ from nominal thicknesses shown in Table 1.

The problem emphasized by our first simulation on the 1829 sample is the major discrepancy between the measured transmittance and the fitted curve if we do not use the appropriate set of optical constants. On Figure 1, we are comparing the measurements with simulations using two different sets of optical constants: the dashed curve (black colored online) is obtained using only CXRO optical constants for Al, Zr and Al_2O_3 while the continuous curve (green colored online) is the result of the combination of Shiles and Palik data for Al (designed as Al-Compilation set in Table 8), Palik data for Al_2O_3, and CXRO data for Zr. The details of simulation parameters are given in Table 2, and details about optical constants are described in the Section 3 of this paper.

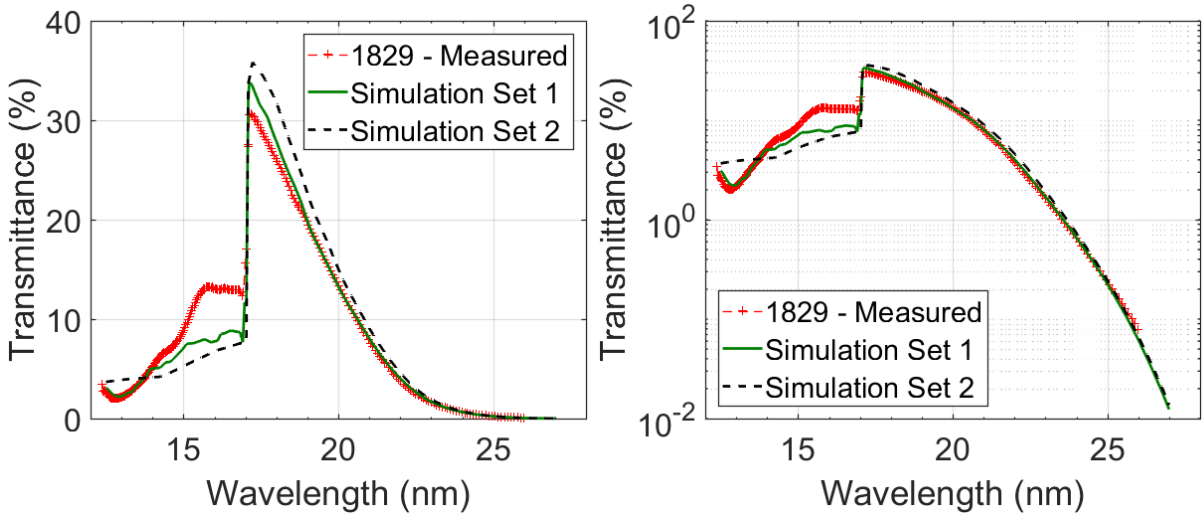

Figure 1. 1829 Al/Zr/Al simulations

Table 2. Simulation parameters of 1829 Filter: Al_2O_3 / Al / Zr / Al / Al_2O_3 (thickness of each layer is given in parenthesis)

1829	*Al (2x45.2 nm), σ = 0.3 nm rms*	*Zr (100.8 nm) σ = 0.3 nm rms*	*Al_2O_3 (2x5 nm) σ = 0.3 nm rms*
Set 1	Al-Compilation	Zr_CXRO	Al2O3_palik
Set 2	Al_CXRO	Zr_CXRO	Al2O3_CXRO

So far, the simulation made with the Set 1 is the best fit we can get for the 1829 Al/Zr filter even if the $L_{2,3}$ absorption edge of Al remains poorly fitted from 14 to 19 nm. For wavelengths above 40 nm, the situation is getting even more complicated as fewer data exist.

On the following Figure 2, we are showing the case of the FSI Engineering Test filter 13396 (see Table 1). Nominal thicknesses are not the same as for the 1829 sample. We found that the optical constants set 1 used to simulate the 1829 filter is also the most appropriate for the 13396 sample. However, we had to adjust thicknesses in our model to get a better fit. According to the simulations, the continuous curve (green colored online) corresponding to the thickness set 1.B is the most accurate compared with the dashed curve standing for the thickness set 1.A (see Table 3). We have to clarify that between 24 and 45 nm, the measured intensity was below noise level so we removed these data from Figure 2.

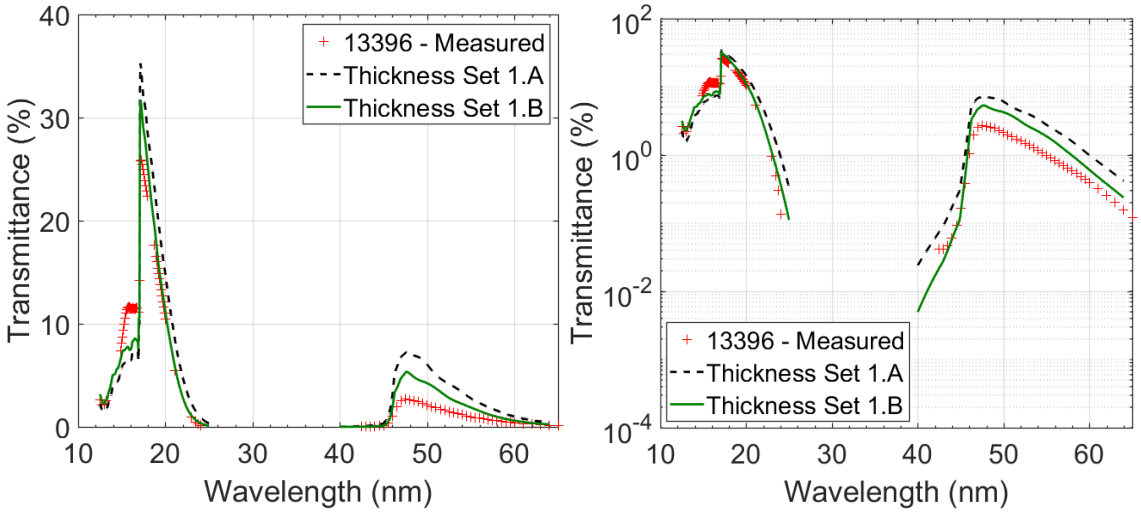

Figure 2. 13396 FSI Engineering Filters - Al/Zr/Al simulations

Table 3. Simulation parameters of 13396 FSI Engineering Filter: Al_2O_3 / Al / Zr / Al / Al_2O_3

13396	*Al σ = 0.3 nm rms*	*Zr σ = 0.3 nm rms*	*Al_2O_3 σ = 0.3 nm rms*
Thickness Set 1.A	49.0 nm | 53.1 nm	92.5 nm	5 nm x2
Thickness Set 1.B	43.3 nm | 45.0 nm	114.5 nm	5 nm x2

Concerning the Al/Mg/Al filter (sample 1906), the $L_{2,3}$ absorption edge of Mg is clearly visible at 25 nm (Figure 3). We are comparing again two sets of optical constants: the dashed curve (black colored online) is obtained using CXRO optical constants for Al, Mg and Al_2O_3 while the continuous curve (green colored online) is obtained using compilation of data for Al and Mg (designed respectively as Al-Compilation and Mg-Compilation sets, see section 3 for more details), and Palik data for Al_2O_3. and the combination by Monica Fernandez-Perea (designed as Mg-Compilation set in Table 8) for Mg. The details of simulation parameters are given in Table 4.

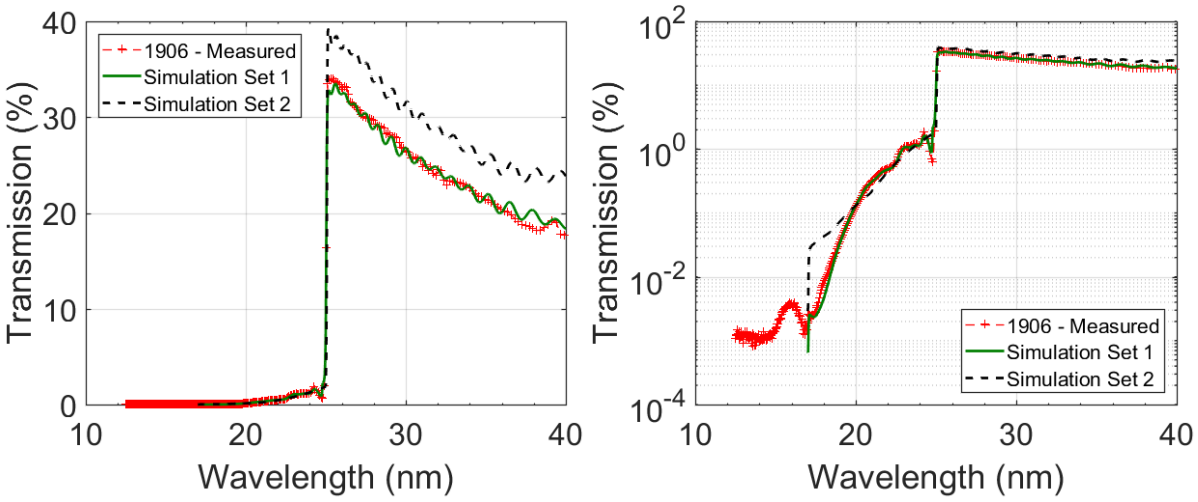

Figure 3. 1906 Al/Mg/Al simulations

Table 4. Simulation parameters of 1906 Filter: Al_2O_3 / Al / Mg / Al / Al_2O_3. Layer thicknesses are given in parenthesis.

1906	*Al (2x65 nm), σ = 0.3 nm rms*	*Mg (32.2 nm) σ = 0.3 nm rms*	*Al_2O_3 (2x5 nm) σ = 0.3 nm rms*
Set 1	Al_Compilation	Mg_Compilation	Al2O3_palik
Set 2	Al_CXRO	Mg_CXRO	Al2O3_CXRO

The Set 1 turns out to be the best choice for the simulation of the 1906 sample. The best results for the two kind of filters (Al/Zr/Al and Al/Mg/Al) have been obtained with the following optical constants data: Al-Compilation, Mg-Compilation, Zr_CXRO and Al2O3_Palik (see section 3 for more details). Weaknesses in the fitted simulations are mainly localized near the absorption edges were the optical constants are sparsely determined. As a whole, the analyses of these filters revealed that aluminum optical constants can be a major source of uncertainties if this material is used around its $L_{2,3}$ edge at 17 nm.

2.2.2. Al/Mo/SiC multilayer mirror – three-component structure

Al/Mo/SiC periodic structures have been developed for Solar Orbiter EUV telescopes (FSI and HRI) in order to reach the highest reflectance possible near normal incidence at 17.4 nm, the Fe X emission line. The sample MP17018 (see Table 1) is similar to HRI coatings but the reflectance has been further improved by increasing the number of periods. The reflectance of sample MP17018 has been measured on the BEAR beamline at the Elettra Synchrotron (Italy) and reaches 58% at 17.4 nm for an incidence angle $\theta = 80°$ (Figure 4), being a higher reflectance than the HRI coating which is 56% at 17.4 nm.

Three simulation sets are compared and illustrated on Figure 4. As the former analyses allowed to conclude about the reliability of the Al-Compilation optical constants set, we managed to test Mo and SiC optical constants on the MP17018 multilayer reflectance data. The details of the simulations are given in Table 5. The continuous curve (green colored online) corresponds to the Set 1 simulation, the dashed curve (black colored online) corresponds to the optical constants set 2 and the dot-and-dashed curve (blue colored online) corresponds to the set 2 without oxide. For the sake of clarity, we do not illustrate other comparative curve for SiC, but its optical constants values are not as divergent as the Mo ones (see Section 3 for details).

Set 1 and set 2 curves mostly overlay on each other meaning that in this wavelength range, values from Tarrio and CXRO optical constant data sets do not show enough difference to definitely choose one of them. However, we can clearly highlight the effect of the SiO_2 top layer as we are comparing the MP17018 set 2 with and without silicon dioxide on the surface. Adding a thin layer of SiO_2 (less than 1 nm) improves significantly the agreement between the measured curve and the simulation in the Bragg peak region. However, the influence of the SiO_2 top layer on the reflectance spectra out of the Bragg peak region is negligible.

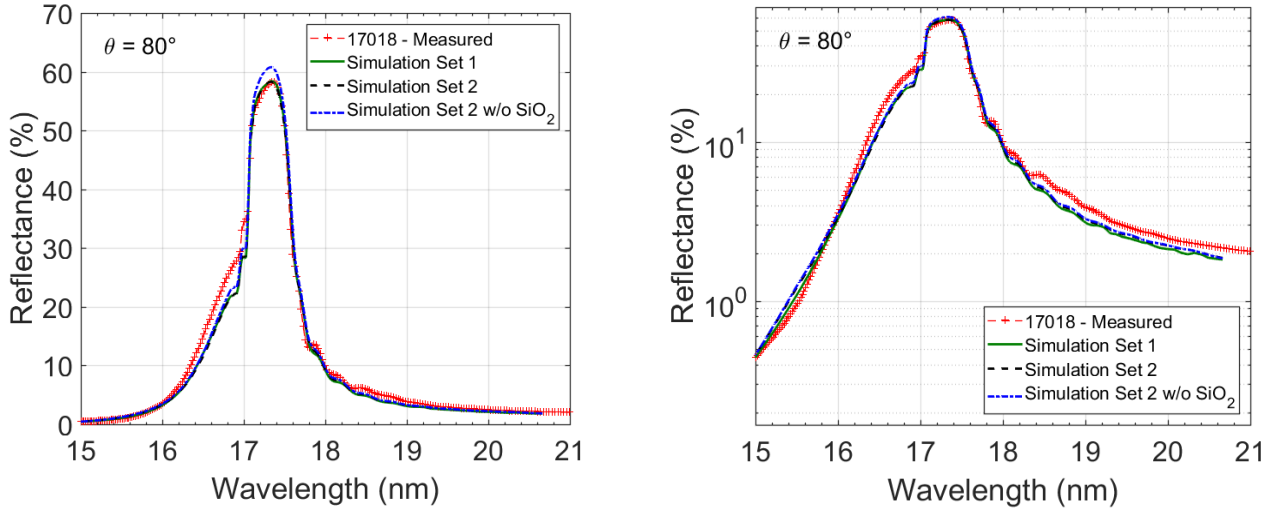

Figure 4. MP17018 Al/Mo/SiC simulations

Table 5. Simulation parameters for MP17018: [Al / Mo / SiC] x 50 + SiC capping layer + SiO_2 top oxide. Layer thicknesses are given in parenthesis.

MP17018	*Al (6.2 nm), σ = 0.3 nm rms*	*Mo (1.8 nm) σ = 0.3 nm rms*	*SiC (0.88 nm + 2.15 nm cap) σ = 0.3 nm rms*	*SiO_2 (0.7 nm) σ = 0.3 nm rms*
Set 1	Al_Compilation	Mo_CXRO	SiC_kortright	aSiO2_CXRO
Set 2	Al_Compilation	Mo_tarrio	SiC_kortright	aSiO2_CXRO
Set 2 w/o SiO_2	Al_Compilation	Mo_tarrio	SiC_kortright	

2.2.3. Al/Mo/B_4C multilayer mirror – three-component structure

Al/Mo/B_4C periodic mirrors (see Table 1) have been developed simultaneously with Al/Mo/SiC and provide high efficiencies with near normal incidence reflectance up to 50% at 21 nm[13] (not shown in this paper) and 42% at 30 nm for an incidence angle θ = 80° (Figure 5).

On Figure 5, we are comparing and illustrating three simulation sets. We managed to test Mo and B_4C optical constants on the MP11024 multilayer reflectance data. It appears that the main issue for fitting the MP11024 data comes from the Mo optical constants. We choose the same B_4C optical constants for the 3 sets because we found that using other B_4C optical constant has no significant effect on the simulated spectra in the spectral range. Indeed, the different tabulated optical constants for B_4C are not as divergent as the Mo ones (see Section 3 for details).

The details of the simulations are given in Table 6. The continuous curve (green colored online) corresponds to the Set 1 simulation, the dashed curve (black colored online) corresponds to the optical constants set 2 and the dotted curve (purple colored online) corresponds to the set 3. From 24 nm to 31 nm, sets 1 and 2 are superimposed with the measured data while the agreement of set 3 with the measured data is poor. None of them fits the measured data above 31 nm, meaning that the tabulated Mo optical constants found in the literature are not reliable above 31 nm (see Section 3 for details). In our case, the best possible fit was achieved with the CXRO optical constants values for Mo.

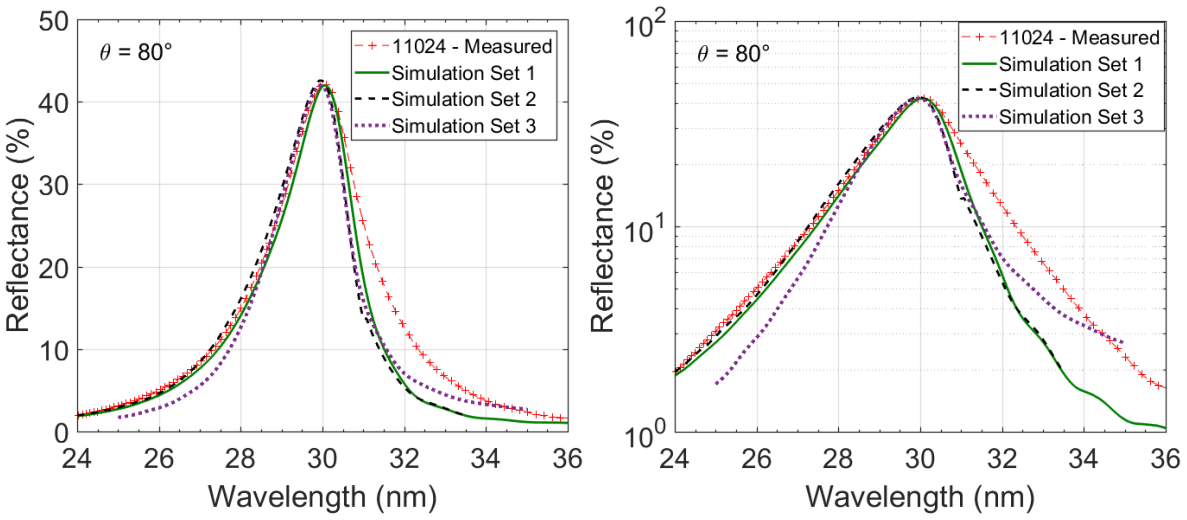

Figure 5. MP11024 Al/Mo/B_4C simulations

Table 6. Simulation parameters for MP11024: [Al/Mo/B4C] x 20. Layer thicknesses are given in parenthesis.

MP11024	*Al (11.3 nm)*	*Mo (1.65 nm)*	*B_4C (3.5 nm)*
Set 1	Al_Compilation	Mo_CXRO	B4C_soufli
Set 2	Al_Compilation	Mo_tarrio	B4C_soufli
Set 3	Al_Compilation	Mo_palik	B4C_soufli

3. OPTICAL CONSTANTS: ISSUES FOR THE EUV RANGE

In this section, we illustrate the different sets of optical constants values found in the literature and on the CXRO website. δ and β values are compared and discussed to conclude about their reliability for EUV optics simulations. In this study, we have worked exclusively on materials optical constants between 10 and 60 nanometers in wavelength to carry out simulations. It is worth noting that we can usually find EUV optical constants defined from 10 nm to 40 nm (CXRO website) for most materials.

The optical constants tabulated in the CXRO database are relying on interpolation between various experimental data sets and calculations for β, and Kramers-Kronig transformation for δ. This means that the δ values determined experimentally by authors are not included in the CXRO database, only the β values are. Furthermore, the CXRO optical constants of compound materials are calculated from the optical constants of their constituent materials (the atomic scattering factors), thus missing near-edge fine structure information that is specific to that compound. Consequently, for compound materials, there is a need to get experimental optical constant data sets measured separately.

First of all, we gathered main references, comments and wavelength range of each optical constants sets found in the literature for Al, Al_2O_3, B_4C, Mg, Mo, SiC and Zr in Table 7. We have calculated the CXRO optical constants of Al, Mg, Mo and Zr from the atomic scattering factors f_1 and f_2 available on the CXRO website. These optical constant sets are plotted and discussed in the following sub-sections. Details about the compilation sets of Al and Mg can be found in Table 8.

Table 7. Different sets of optical constants for Al, Al_2O_3, B_4C, Mg, Mo, SiC and Zr

Material	File Name	Range (nm)	References/Comments
Al	Al_CXRO	0.042 – 41	CXRO (2018) includes β values from Gullikson et al.[14]
	Al_Palik	16.53 – 1239.8	Palik (1985)[8]
	Al_Shiles	1.24 – 130.51	Shiles et al. in [15]
Al_2O_3	Al2O3_CXRO	0.042 – 41	CXRO (2018)
	Al2O3_hagemann	0.77 – 137.76	Hagemann et al. in [15]
	Al2O3_Palik	12.4 - 24996	Palik (1991)[16]
B_4C	B4C_CXRO	0.042 – 41	CXRO (2018)
	B4C_Blumenstock	40.6-200	Blumenstock et al (1995) [17]
	B4C_soufli	1.6 – 60	Soufli et al (2008) DC-sput.[18]
	B4C_tarrio	7.2-30.1	Tarrio et al (1998) in-situ sput. [7]
Mg	Mg_CXRO	0.042 – 41	CXRO (2018) includes β values from Gullikson et al. (1994) [14] and [19]
	Mg_Vidal	0.95 – 49.6	Manuela Vidal-Dasilva at ALS [19]
	Mg_Daude	51.54 – 114.50	Daude (1969) [20]
	Mg_hagemann	0.025 – 17711.4	Hagemann (1975) [21]
Mo	Mo_CXRO	0.042 – 41	CXRO (2018) includes β values from Soufli and Gullikson (1998)[22] and Tarrio (1998)[7]
	Mo_tarrio	8.8 – 33.6	Tarrio et al (1998)[7] in-situ sput.
	Mo_palik	6.2 – 123980	Palik (1985)[8]
SiC	SiC_CXRO	0.042 – 41	CXRO (2018)
	SiC_kortright	2.4 – 121.6	Kortright and Windt (1988) [23]
	SiC_larruquert	6.2 – 123.98	Larruquert et al. (2011)[24]
Zr	Zr_CXRO	0.012 – 64.92	CXRO (2018)
	Zr_lynch	41.3 – 137.8	Lynch et al. (DESY) (1981)[8]
	Zr_windt	2.4 – 121.6	Windt et al. (1988)[25]

Table 8. Aluminum and Magnesium compilation sets

File Name	Wavelength Range (nm)	References / Comments
Al - Compilation	1.24 – 1239.8	Shiles until 19 nm, then Palik + replacing of k absorption coefficients in Shiles by Palik ones
Mg - Compilation	0.95 – 114.5	Concatenation of: 0.95 – 49.6 nm: Manuela Vidal-Dasilva at ALS [19] 51.54 – 114.5 nm: Daude 1969 [20]

3.1. Aluminum & Aluminum oxide

Aluminum is an essential material for transmission filters in EUV space missions. Moreover, it has been recently used in EUV multilayer optics [13,26,27]. We noticed differences around 17 nm, the Al $L_{2,3}$-edge, while comparing Palik, Shiles and CXRO data on Figure 6.

Concerning the CXRO data (continuous curve, blue-colored online), which we have calculated from the atomic scattering factors available online, β values are available on the whole spectral range of interest, but δ values stop at 41 nm. We can see on Figure 6 that Al CXRO data are missing the Al near-edge fine structure information below 17 nm and that they differ significantly from Palik and Shiles sets. Palik (empty red-colored circles) and Shiles (green dots) values are consistent and we managed to combine them to improve the accuracy of our Al thin film simulations. Shiles values provide well defined structures below the $L_{2,3}$-edge as we can see the Al fine structure at the edge. However, a stepwise progression appears above this edge on the absorption coefficient due to an approximation to the third decimal existing in these data. Replacing the β values above 17 nm by the corresponding ones in the Palik data compensates this effect and gives a better precision. On the other hand, the Palik data show a poor spectral resolution below the $L_{2,3}$-edge (no fine structure and disagreement between data and simulations below 17 nm). From filters and mirrors simulations in Section 2 we can conclude that the above-mentioned combination of Palik and Shiles values, designed as Al-Compilation set, is the most adapted in the EUV range.

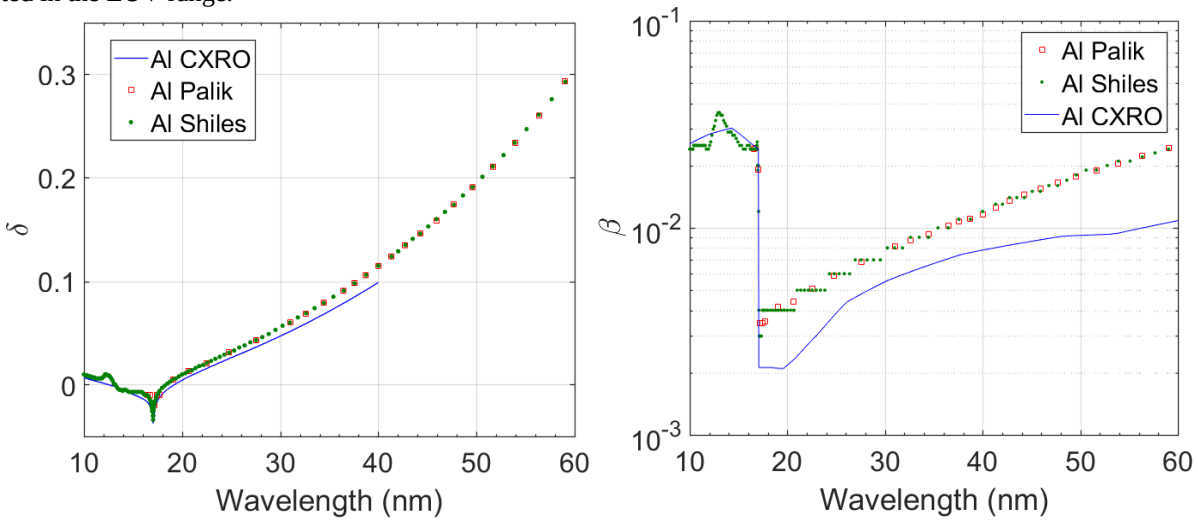

Figure 6. Aluminum optical constants

Used as a surface layer, Al oxidizes to create an average 5 nm thick Al_2O_3 layer. In EUV optical systems, such an oxide is not negligible as it may induce a loss in efficiency, if not taken into account [8]. Al_2O_3 optical constants from the CXRO database (continuous curve, blue-colored online) are very different from the Hagemann (full diamond markers, orange-colored online) and Palik (empty diamond markers) values, as they are calculated values missing the matrix effect (Figure 7). As a consequence, the $L_{2,3}$ absorption edge of aluminum still appears at 17.4 nm on CXRO data while it is shifted in the Hagemann and Palik measured data. As illustrated in Section 2, Al_2O_3 optical constants from Palik provide the most accurate fit of experimental transmittance.

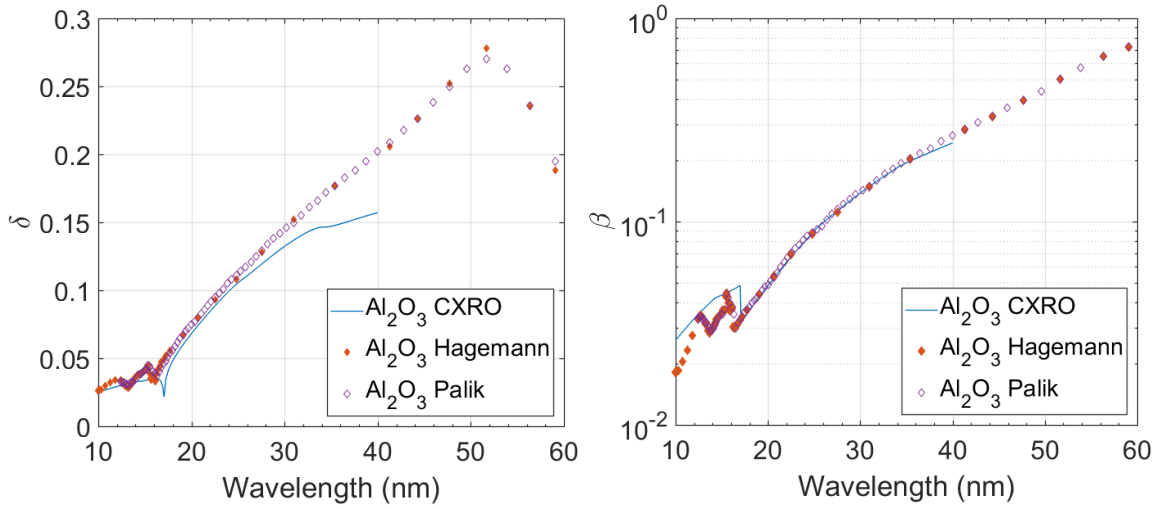

Figure 7. Aluminum Oxide Al_2O_3 optical constants

3.2. Zirconium

Zirconium is another interesting thin film for EUV optics [9,27] and, like Al, another essential material for transmission filters in EUV space missions. Unfortunately, we observe major discrepancies between different sets of data as illustrated in Figure 8. While significant differences in reported CXRO (continuous curve, blue-colored online) and Windt (diamond markers, green-colored online) β values exist between 10 and 20 nm, the situation is even worse above 40 nm where its value can vary by a factor of ten with Lynch values starting at 41.3 nm (diamond markers, purple-colored online). On the other hand, CXRO and Windt δ coefficients seem consistent until about 40 nm but major divergences occur above this limit. According to these data and to the simulations presented in Section 2 for Al/Zr filters, CXRO optical constants appear to be the best choice for this material in the EUV range with a good reliability between 10 and 40 nm.

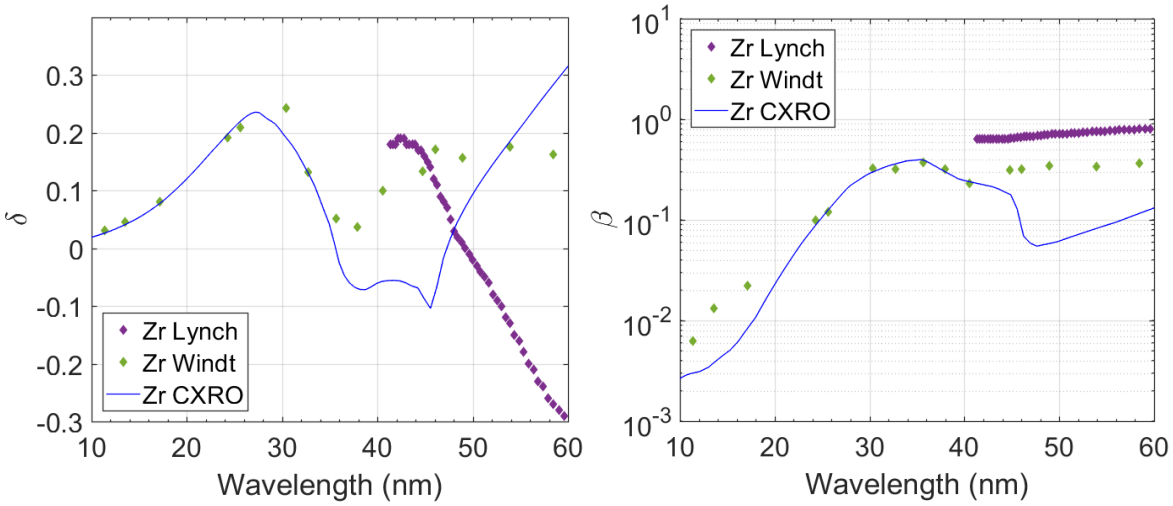

Figure 8. Zirconium optical constants

3.3. Magnesium

Magnesium has been used in several filters and multilayer mirrors in EUV optics for space applications [9,19,28]. Mg-based multilayers present superior reflective performance. They were prevented from use in EUV multilayer mirrors for space application due to corrosion, but they have a newfound popularity due to the development of corrosion barriers[29].

On Figure 9, CXRO optical constants values (continuous curve, blue-colored online) include the absorption coefficients β of Mg-Compilation (dotted curve, red-colored online). However, CXRO δ coefficients are differing from Mg-Compilation above 25 nm and the difference increases with the wavelength. This divergence may be due to differences in the set of β values used for the calculation of δ via Kramers-Kronig raltion. Hagemann curves (full diamond markers, purple-colored online) exhibit the similar shape as CXRO and Mg-Compilation sets but its values are higher on the whole range of wavelength, with an increasing divergence above 25 nm for both δ and β coefficients.

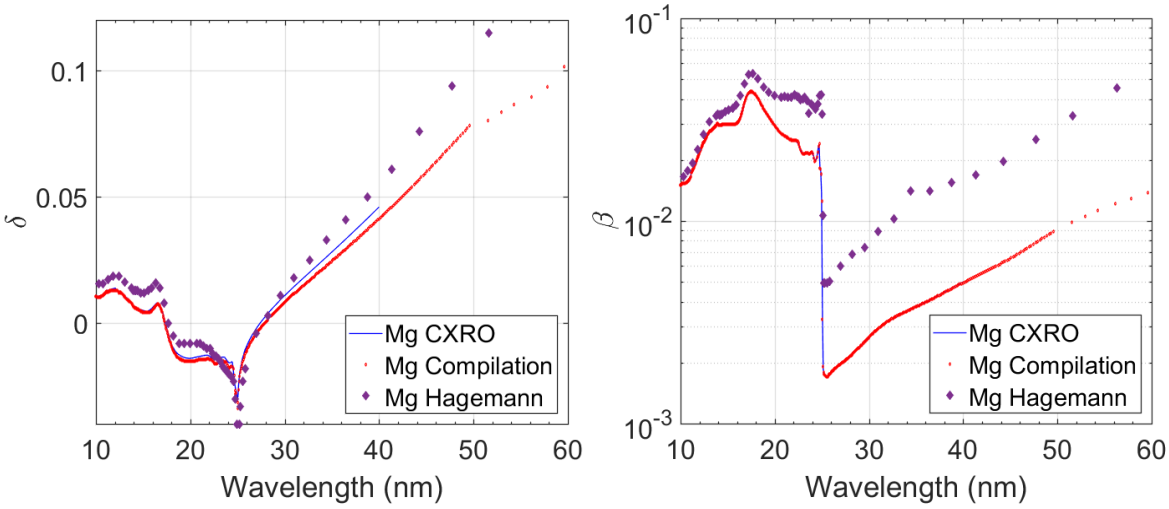

Figure 9. Magnesium Optical Constants

According to simulations done with Al/Mg/Al filters (see Section 2.2), Mg optical constants compiled from Vidal-Dasilva and Daude (see Table 8) provide the most accurate and reliable values from 17 nm to 40 nm.

3.4. Molybdenum

Molybdenum is another well-known material for its performances in the EUV region when combined with Silicon. Mo/Si is one of the earliest developed and the most studied and employed EUV multilayer. Mo/Si periodic mirrors have been successfully used for on-board telescopes such as SOHO/EIT [1], STEREO/EUVI [30], SUVI/GOES [31] and SDO/AIA[32] or to detect iron and helium emission lines from different parts of the solar atmosphere. More recently, Mo has also been used in Al-based multilayers, which have been developed and successfully deposited on two EUV telescopes for Solar Orbiter[9].

Despite these applications, we still find discrepancies between the different sets of Mo optical constants (Figure 10) which have strong impact on simulations as seen in the analyses of three-component multilayer mirrors (see Section 2). CXRO values (continuous curve, blue-colored online) include Tarrio absorption coefficients β (full markers, red-colored online). As Tarrio set stops at 33 nm, CXRO values have been extended with more calculations using Palik absorption coefficients (empty black markers). Major discrepancies appear from 30 nm concerning the absorption coefficient β which corresponds to the N_2 absorption edge of Mo, but start earlier at 21 nm for δ. Analyses of MP17018 and MP11024 in Section 2 have shown that the existing Tarrio and CXRO Mo optical constants before 30 nm, which corresponds to the N_2 absorption edge of Mo, are quite accurate for simulations. Above this wavelength and up to 60 nm, existing optical constants sets are not enough reliable for accurate simulations.

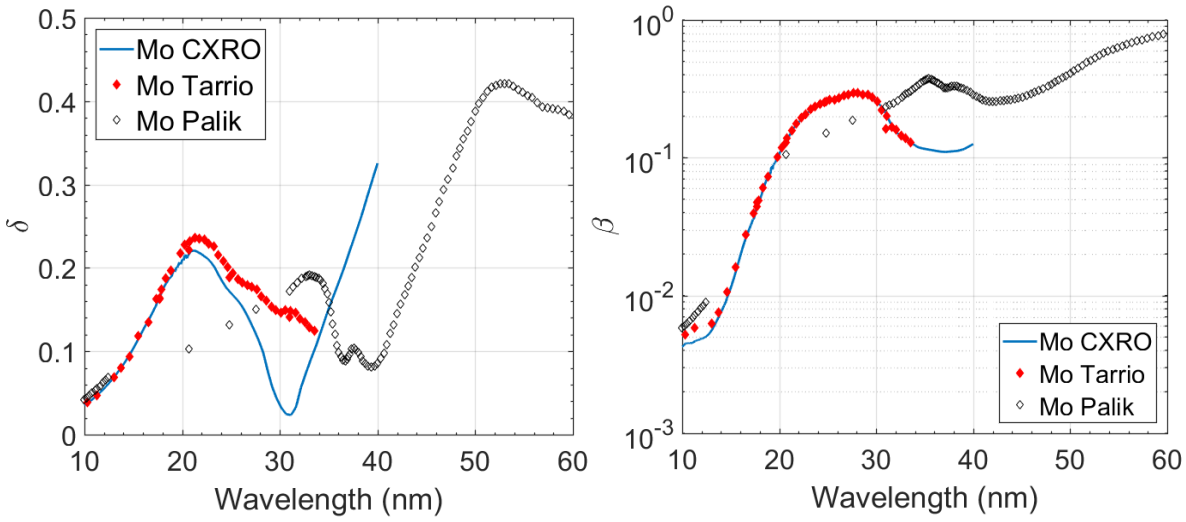

Figure 10. Molybdenum Optical Constants

3.5. Silicon Carbide and Boron Carbide

Silicon carbide and boron carbide thin films have been used in the design of many multilayer EUV/X-ray mirrors for space applications[3,32–34] . SiC and B_4C are frequently used as components in multilayer coatings, but also as single-layer coatings for EUV space applications due to their significant reflectance as single layers at wavelengths above 50 nm[35]. SiC and B_4C optical constants found in the literature do not show major discrepancies compared to most of the materials discussed in this paper (Figure 11 and Figure 12 for SiC and B_4C respectively). Nevertheless, differences appear starting at 40 nm for the SiC δ coefficients and starting at 30 nm for B_4C.

On Figure 11, three sets are compared: Kortright & Windt (full diamond markers, green-colored online), Larruquert (dotted curve, red-colored online) and CXRO (continuous curve, blue-colored online) optical constants values (see Table 7). Analyses in Section 2 showed that SiC Kortright values provided reliable results for EUV optics simulations from 15 to 21 nm but further analyses would be interesting to conclude on the reliability of SiC optical constants above 40 nm.

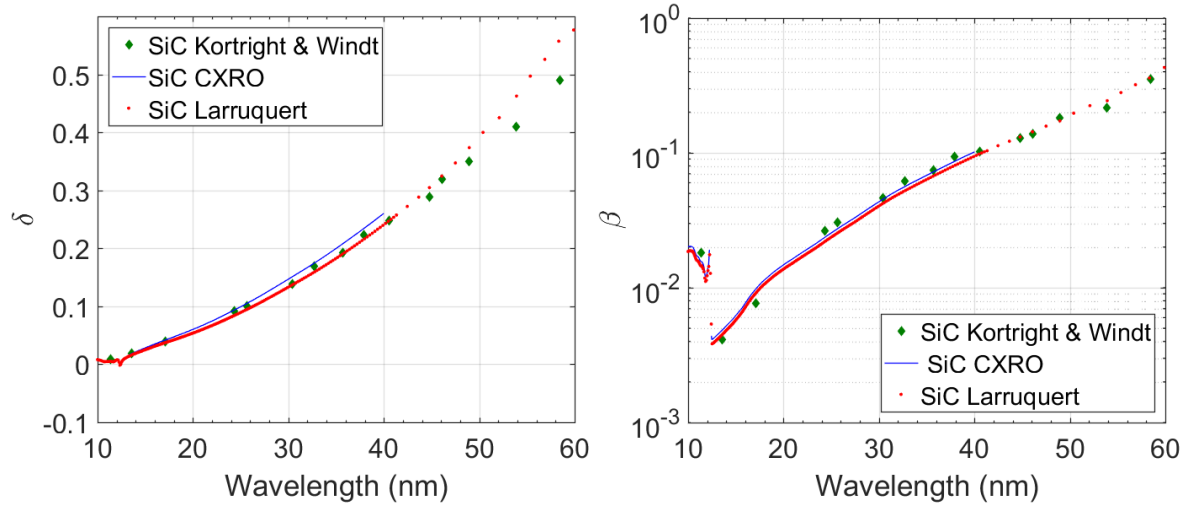

Figure 11. Silicon Carbide SiC optical constants

On Figure 12 concerning B_4C, four sets are compared: Soufli (dot-dashed curve, red-colored online), Tarrio (full diamond markers, black-colored online), Blumenstock (full square markers, blue-colored online), and CXRO (continuous curve, blue-colored online) optical constants values (see Table 7). Analyses in Section 2 showed that B_4C Soufli values provides reliable results for EUV optics simulations.

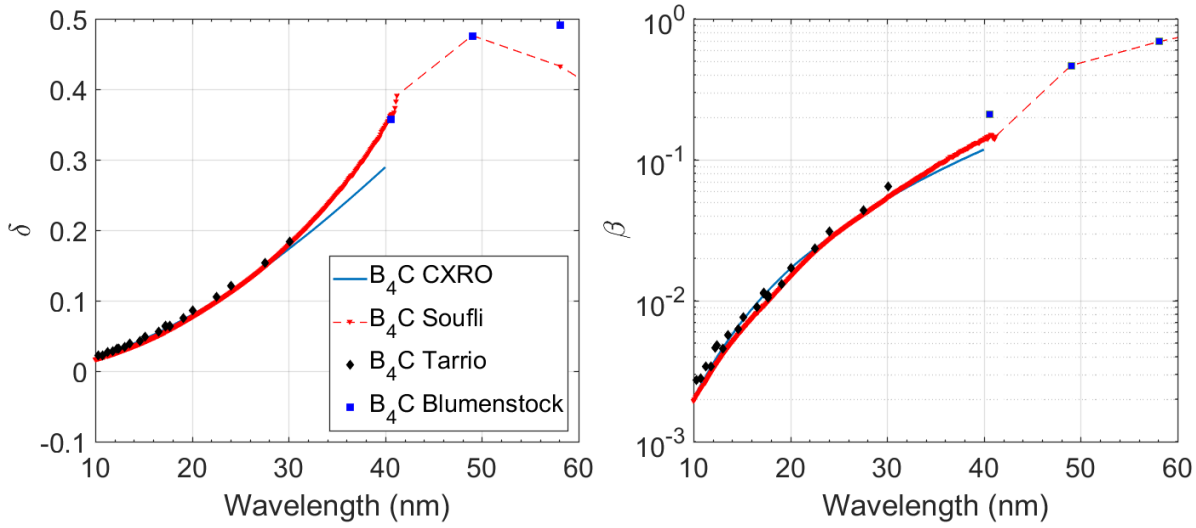

Figure 12. Boron Carbide B_4C optical constants

The development of SiC-based multilayer above 40 nm, as well as B_4C-based multilayers above 30 nm, would need further investigations to test the reliability of existing sets of data and/or new optical constants measurements.

4. DISCUSSION

From the simulations of filters and multilayer mirrors and the state-of-the-art on optical constants shown in this paper we are able to draw some conclusions about the reliability of optical constant data sets between 10 and 60 nm in the EUV range.

The following figure (Figure 13) is a graphical summary concerning the tabulated EUV optical constants values tested in this study for aluminum, aluminum oxide, boron carbide, magnesium, molybdenum, silicon carbide and zirconium. Every horizontal line stands for a set of optical constants defined over the wavelength range considered and they are grouped by material. Discontinued lines stand for the less accurate values according to our EUV simulations. In general, we have seen that the CXRO optical constants give a good but limited estimation of the response in the EUV wavelength range from 10 nm to 41 nm. CXRO optical constant sets are usually not available above 41 nm. Unbroken thin lines in Figure 13 are reliable optical constants with quite well identified weaknesses. The thickest unbroken lines are the most accurate values so far as the best simulations have been achieved with these sets. However, independently from the reliability of each set, absorption edges are always at the root of major discrepancies ($L_{2,3}$-edges of Si, Al, Mg and N_2-edges of Mo and Zr are shown in Figure 13).

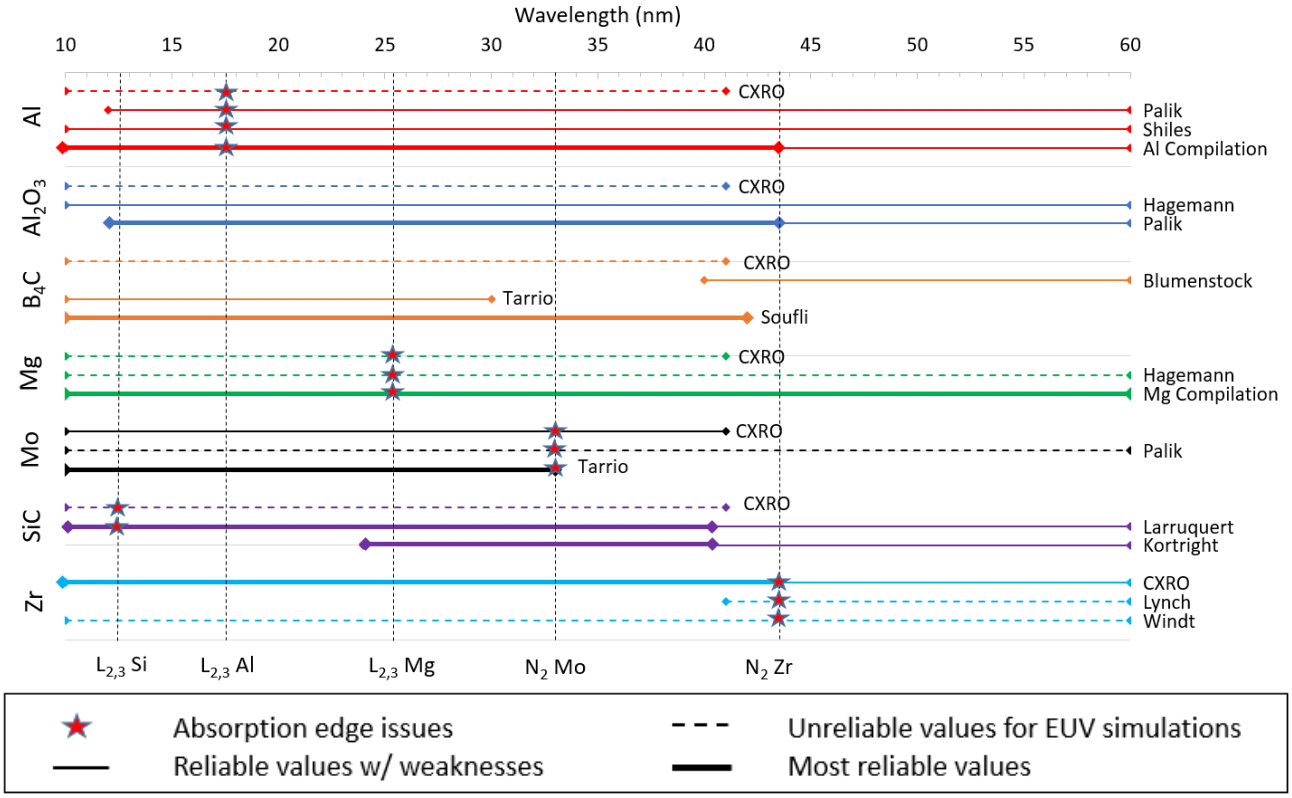

Figure 13. Graphical representation of different tabulated optical constants and main conclusions

5. CONCLUSIONS

As a whole, we have identified sensitive wavelength regions where optical constants of thin film materials are inaccurate. Molybdenum and Zirconium are interesting and well-known materials for space applications but they still show major discrepancies over the 10-60 nm range. New measurements on these materials are becoming a requirement to improve simulations such as the ones shown in this paper. Aluminum optical constants allow achieving good fitting results even if weaknesses persist in the vicinity of its $L_{2,3}$-absorption edge. Perhaps more measurements around 17 nm would improve these results.

As well as the materials above, optical constants of oxides are not well known in the EUV range and they can still have a major influence on the efficiency of our multilayer coatings as illustrated in this paper with Al_2O_3 (see Section 3.1). As they naturally appear once the coating is exposed to air and often grow in time, their properties must be known in order to anticipate and avoid any loss in efficiency of the optical coating.

The good agreement between experimental and simulated data using these optical constants will enable the optimization of new multilayer coatings for the development of high efficiency instruments in solar physics. So far, the state-of-the-art of optical constants in the EUV range from 10 nm to 60 nm combined with simulations allowed the identification of several wavelength regions which need more measurements. Further measurements in the region from 40 nm to 60 nm and above could improve our understanding of every material mentioned in this paper.

ACKNOWLEDGMENTS

The multilayer mirrors were deposited on CEMOX (Couches Minces pour l'Optique X), a platform of LUMAT federation (CNRS FR2764). This work was supported by the French Space Agency (CNES), by the French Research Agency (project n°ANR3113EQPX30005) and by the Jean d'Alembert fellowship program from Université Paris-Saclay. This work was performed under the auspices of the U.S. Department of Energy by Lawrence Livermore National Laboratory under Contract No. DE-AC52-07NA27344.

REFERENCES

[1] Delaboudiniere, J.-P. *et al.* EIT: extreme-ultraviolet imaging telescope for the SOHO mission. in *The SOHO Mission* 291–312 (Springer, 1995).

[2] Delmotte, F. *et al.,* "B4C/Mo/Si multilayers for 20-40 nm wavelengths: application to broadband mirrors," in *Advances in Optical Thin Films II* **5963,** 59631V (International Society for Optics and Photonics, 2005).

[3] Delmotte, F. *et al.,* "Development of multilayer coatings for solar orbiter EUV imaging telescopes," in (eds. Fineschi, S. & Fennelly, J.) 88620A (2013). doi:10.1117/12.2036050

[4] Windt, D. L., "EUV multilayer coatings for solar imaging and spectroscopy," in *Solar Physics and Space Weather Instrumentation VI* **9604,** 96040P (International Society for Optics and Photonics, 2015).

[5] Windt, D. L., "IMD—Software for modeling the optical properties of multilayer films," *Comput. Phys.* **12,** 360 (1998).

[6] Uspenskii, Y. A. *et al.,* "Efficient method for the determination of extreme-ultraviolet optical constants in reactive materials: application to scandium and titanium," *JOSA A* **21,** 298–305 (2004).

[7] Tarrio, C., Watts, R. N., Lucatorto, T. B., Slaughter, J. M. & Falco, C. M., "Optical constants of in situ-deposited films of important extreme-ultraviolet multilayer mirror materials," *Appl. Opt.* **37,** 4100–4104 (1998).

[8] Palik, E.D., [Handbook of optical constants of solids] (Acad. Press, 1985).

[9] Halain, P. *et al.,* "The extreme ultraviolet imager of solar orbiter: optical design and alignment scheme," in *SPIE Optical Engineering + Applications* (ed. Fineschi, J., S; Fennelly) **9604,** 96040H (SPIE-INT SOC OPTICAL ENGINEERING, 1000 20TH ST, PO BOX 10, BELLINGHAM, WA 98227-0010 USA, 2015).

[10] Gautier, J. *et al.,* "Study of normal incidence of three-component multilayer mirrors in the range 20–40 nm," *Appl. Opt.* **44,** 384–390 (2005).

[11] Auchère, F. *et al.,* "HECOR: a HElium CORonagraphy aboard the Herschel sounding rocket," in *Solar Physics and Space Weather Instrumentation II* **6689,** 66890A (International Society for Optics and Photonics, 2007).

[12] Idir, M., Mercere, P., Moreno, T. & Delmotte, A., "Technical Report: Metrology and Test Beamline at SOLEIL," *Synchrotron Radiat. News* **19,** 18–23 (2006).

[13] Meltchakov, E. *et al.,* "Single and multi-channel Al-based multilayer systems for space applications in EUV range," in *Damage to VUV, EUV, and X-ray Optics IV; and EUV and X-ray Optics: Synergy between Laboratory and Space III* **8777,** 87771C (International Society for Optics and Photonics, 2013).

[14] Gullikson, E. M., Denham, P., Mrowka, S. & Underwood, J. H. Absolute photoabsorption measurements of Mg, Al, and Si in the soft-x-ray region below the L2,3 edges. *Phys. Rev. B Condens. Matter* **49,** 16283–16288 (1994).

[15] Weaver, J. H., Krafka, C., Lynch, D. W. & Koch, E. E. [Physik Daten, Physics Data: Optical Properties of Metals], **Vol. 18-1, Vol. 18-2,** (1981).

[16] Palik, E. D., [Handbook of Optical constants of solids II], (Acad. Press, 1991).

[17] Blumenstock, G. M., Keski-Kuha, R. A. M. & Ginter, M. L. , "Extreme ultraviolet optical properties of ion-beam-deposited boron carbide thin films," in *X-Ray and Extreme Ultraviolet Optics* **2515,** 558–565 (International Society for Optics and Photonics, 1995).

[18] Soufli, R., Aquila, A. L., Salmassi, F., Fernández-Perea, M. & Gullikson, E. M., "Optical constants of magnetron-sputtered boron carbide thin films from photoabsorption data in the range 30 to 770 eV," *Appl. Opt.* **47,** 4633–4639 (2008).

[19] Vidal-Dasilva, M., Aquila, A. L., Gullikson, E. M., Salmassi, F. & Larruquert, J. I., "Optical constants of magnetron-sputtered magnesium films in the 25–1300 eV energy range," *J. Appl. Phys.* **108,** 063517 (2010).

[20] Daudé, A., Savary, A., Jezequel, G. & Robin, M. S., "Determination des constantes optiques du magnesium entre 500 et 1400 A," *Opt. Commun.* **1,** 237–240 (1969).

[21] Hagemann, H.-J., Gudat, W. & Kunz, C., "Optical constants from the far infrared to the x-ray region: Mg, Al, Cu, Ag, Au, Bi, C, and Al2O3," *JOSA* **65,** 742–744 (1975).

[22] Soufli, R. & Gullikson, E. M. Absolute photoabsorption measurements of molybdenum in the range 60–930 eV for optical constant determination. *Appl. Opt.* **37,** 1713 (1998).

[23] Kortright, J. B. & Windt, D. L., "Amorphous silicon carbide coatings for extreme ultraviolet optics," *Appl. Opt.* **27,** 2841–2846 (1988).
[24] Larruquert, J. I. *et al.,* "Self-consistent optical constants of SiC thin films," *JOSA A* **28,** 2340–2345 (2011).
[25] Windt, D. L. *et al.,* "Optical constants for thin films of Ti, Zr, Nb, Mo, Ru, Rh, Pd, Ag, Hf, Ta, W, Re, Ir, Os, Pt, and Au from 24 A to 1216 A," *Appl. Opt.* **27,** 246–278 (1988).
[26] Meltchakov, E. *et al.,* "Development of Al-based multilayer optics for EUV," *Appl. Phys. A* **98,** 111 (2010).
[27] Zhong, Q. *et al.,* "Enhancement of the reflectivity of Al/Zr multilayers by a novel structure," *Opt. Express* **21,** 14399 (2013).
[28] Fernández-Perea, M. *et al.,* "Triple-wavelength, narrowband Mg/SiC multilayers with corrosion barriers and high peak reflectance in the 25-80 nm wavelength region," *Opt. Express* **20,** 24018–24029 (2012).
[29] Soufli, R. *et al.,* "Spontaneously intermixed Al-Mg barriers enable corrosion-resistant Mg/SiC multilayer coatings," *Appl. Phys. Lett.* **101,** 043111 (2012).
[30] Wuelser, J.-P. *et al.,* "EUVI: the STEREO-SECCHI extreme ultraviolet imager," in (eds. Fineschi, S. & Gummin, M. A.) 111 (2004). doi:10.1117/12.506877
[31] Martínez-Galarce, D. S. *et al.,* "Multisegmented, multilayer-coated mirrors for the Solar Ultraviolet Imager," *Opt. Eng.* **52,** 095102 (2013).
[32] Lemen, J. R. *et al.,* "The Atmospheric Imaging Assembly (AIA) on the Solar Dynamics Observatory (SDO)," *Sol. Phys.* **275,** 17–40 (2012).
[33] Windt, D. L., Gullikson, E. M. & Walton, C. C., "Normal-incidence reflectance of optimized W/B4C x-ray multilayers in the range 1.4 nm < l < 2.4 nm," 3 (2002).
[34] Soufli, R. *et al.,* "Development and testing of EUV multilayer coatings for the atmospheric imaging assembly instrument aboard the Solar Dynamics Observatory," in *Solar Physics and Space Weather Instrumentation* **5901,** 59010M (International Society for Optics and Photonics, 2005).
[35] Blumenstock, G. M. & Keski-Kuha, R. A., "Ion-beam-deposited boron carbide coatings for the extreme ultraviolet," *Appl. Opt.* **33,** 5962–5963 (1994).